Electronic Supplementary Information (ESI)

## Enhanced Synergistic Catalysis by Novel Triple-phase Interfaces Design of NiO/Ru@Ni for Hydrogen Evolution Reaction

Chenglin Zhong,[‡a] Qingwen Zhou,[‡a] Shengwen Li,[a] Lin Cao,[a] Jiachen Li,[b] Zihan Shen,[a] Haixia Ma,[b] Jianguo Liu,[a] Minghui Lu[a] and Huigang Zhang*[a]
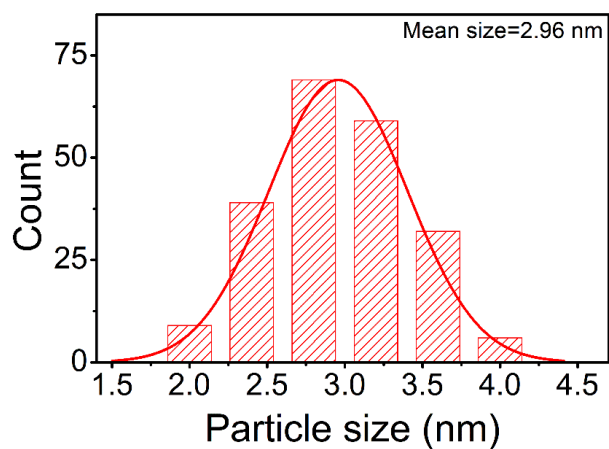
[a]National Laboratory of Solid State Microstructures, College of Engineering and Applied Sciences, and Collaborative Innovation Center of Advanced Microstructures, Nanjing University, Nanjing 210093, P.R. China.
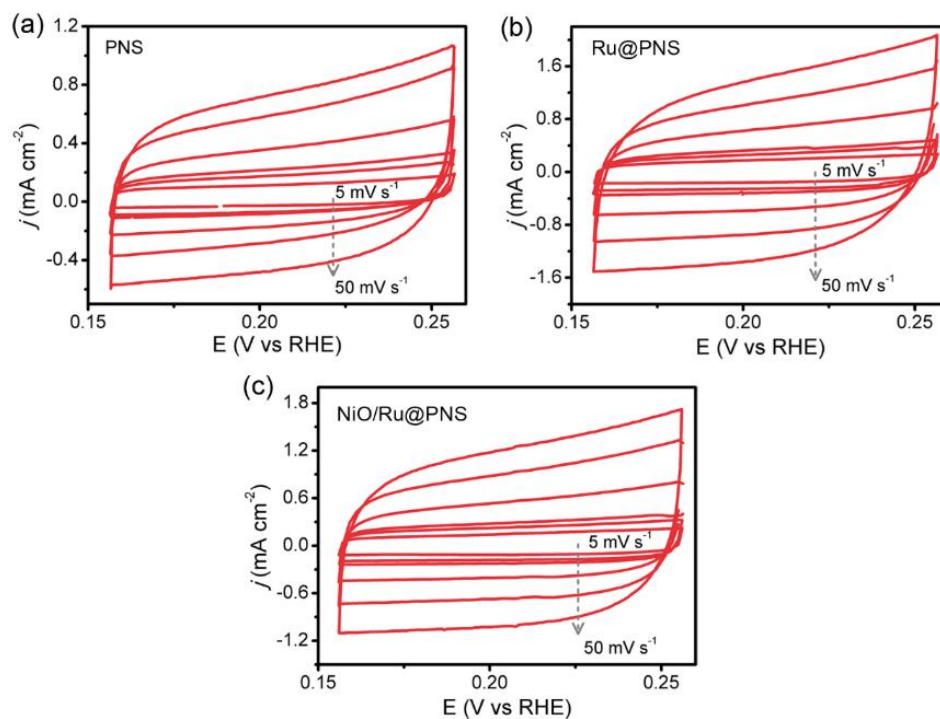*E-mail:hgzhang@nju.edu.cn

[b]Department of Chemical Engineering, Northwest University, Xi'an 710069, P. R. China
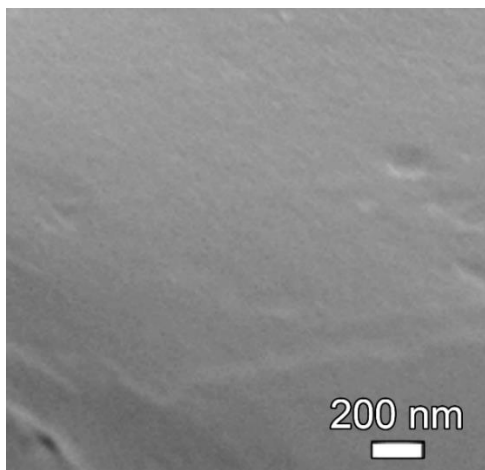
Fig. S1 SEM images of PNS.

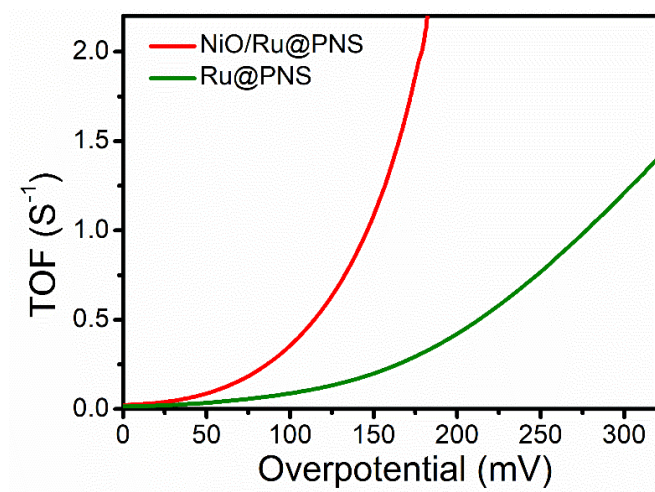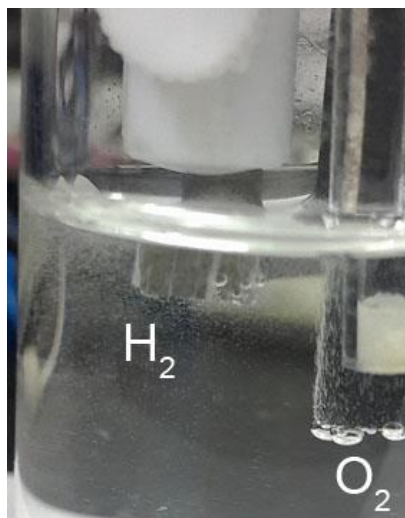**Fig. S2** The particle size distribution of Ru nanoparticles in NiO/Ru@PNS.

Fig. S3 Cyclic voltammograms of as-prepared catalysts at different scanning rates of 5, 8, 10, 20, 35, and 50 mV s^{-1}: (a) PNS, (b) Ru@PNS, and (c) NiO/Ru@PNS.

Fig. S4 TOFs of NiO/Ru@PNS and Ru@PNS at different overpotential.

Fig. S5 Optical photograph shows the bubble generation at -200 mA cm^{-2}.
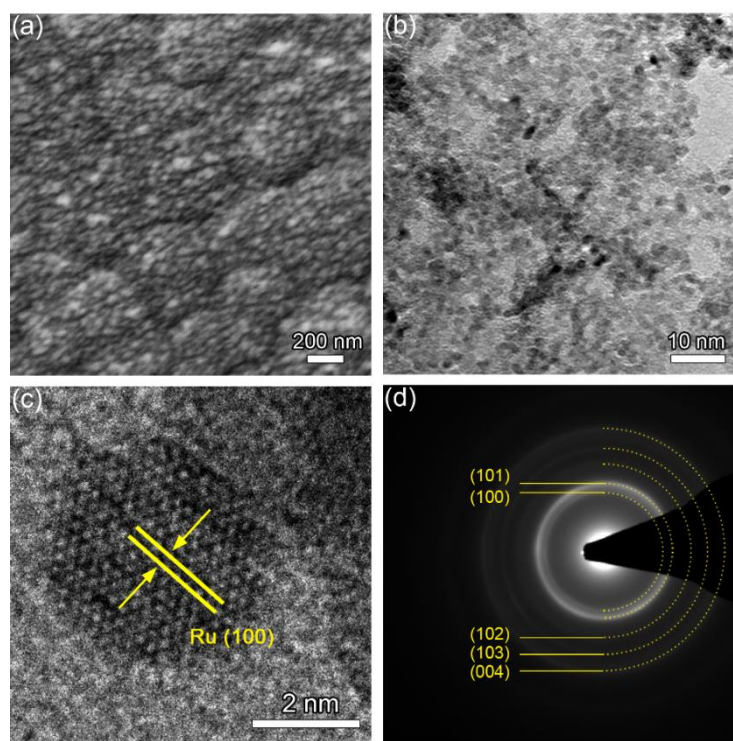
Fig. S6 (a) SEM image of the NiO/Ru@PNS electrode surface after 80 h electrolysis. (b) TEM image, (c) HRTEM image, and (d) SAED of the obtained Ru nanoparticles from the NiO/Ru@PNS sample after the 80 h electrolysis.
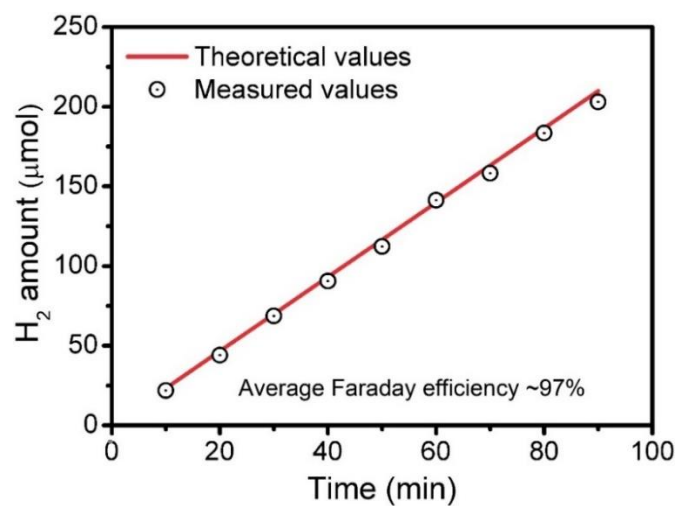
Fig. S7 Faradaic efficiency of NiO/Ru@PNS for HER.
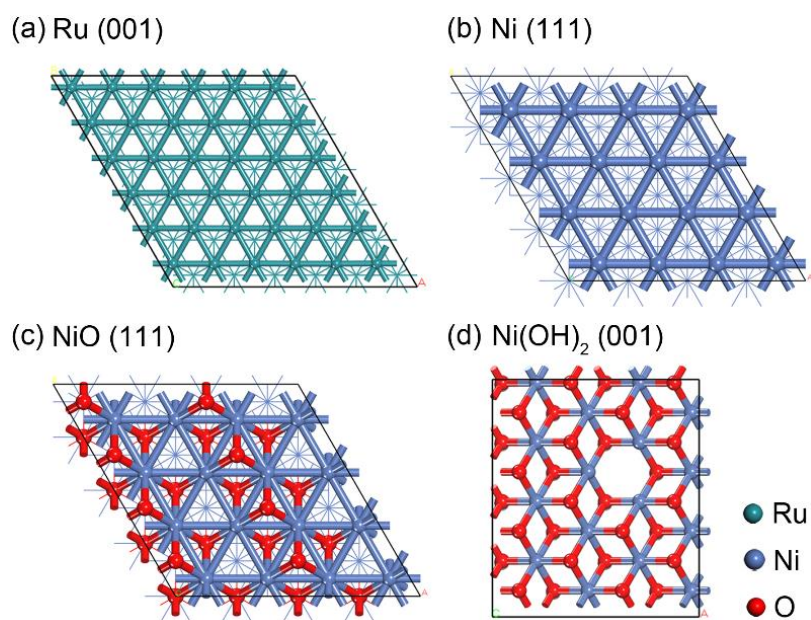
Fig. S8 The as-built catalyst models for the DFT calculations.
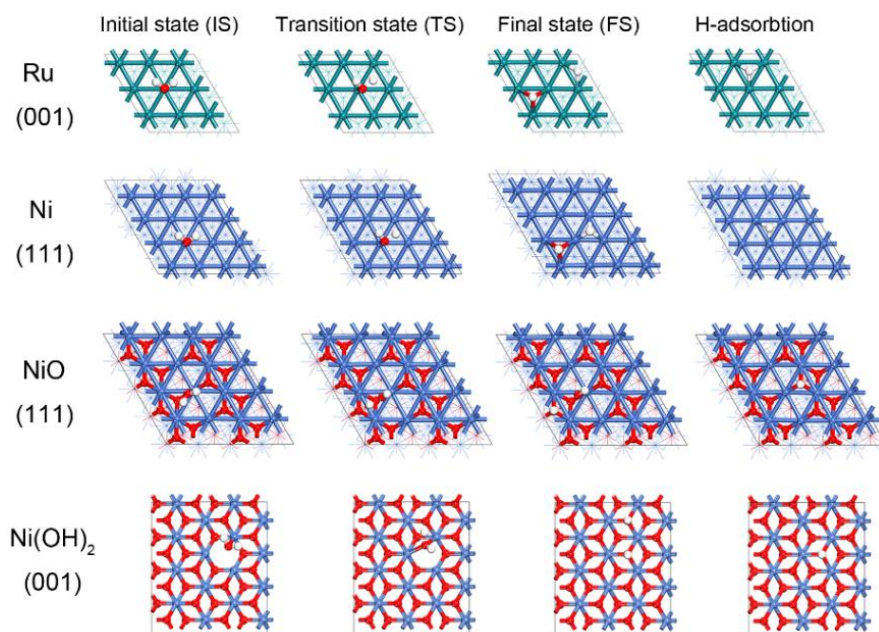
Fig. S9 Initial state (IS), transition state (TS), final state (FS) for water dissociation, and H adsorption on Ru (001), Ni (111), NiO (111), and Ni(OH)$_2$ (001) facets, respectively.
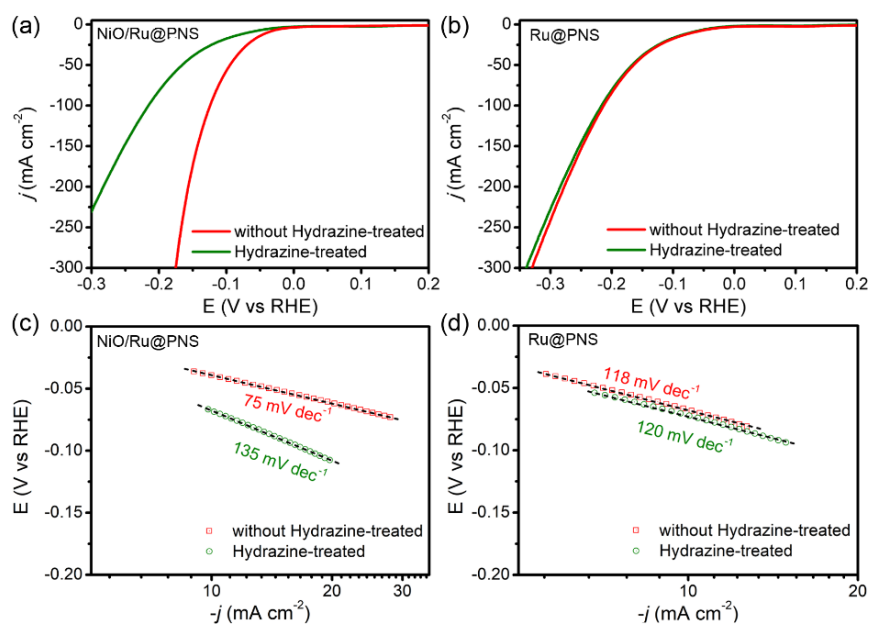
Fig. S10 LSV polarization curves of (a) NiO/Ru@PNS and (b) Ru@PNS before and after the hydrazine reduction process. Corresponding Tafel plots of (c) NiO/Ru@PNS and (d) Ru@PNS before and after the hydrazine reduction process.
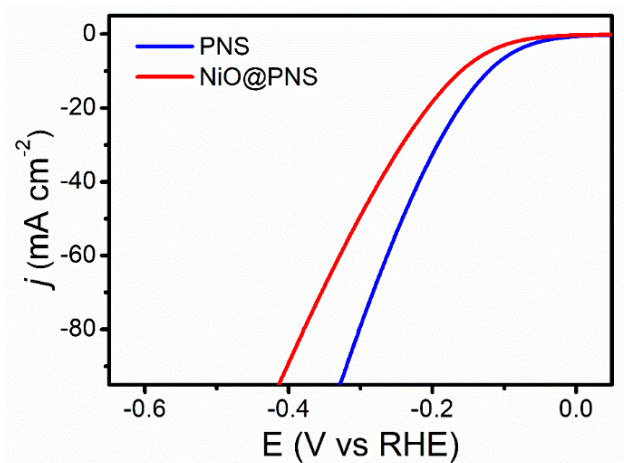
Fig. S11 LSV polarization curves of PNS before and after the in-situ electro-oxidation process.

Table S1. Comparison of electrocatalytic HER activity of most recently reported HER catalysts in alkaline media.

Catalysts	Current density	Corresponding overpotential	Tafel slope (mV dec^{-1})	Stability test (h)	Ref.

	j (mA cm^{-2})	η (mV)			
Cu NDs/Ni$_3$S$_2$ NTs-CFs	−10	128	76.2	30	1
	−50	212			
	−100	260			
MoS$_2$/NiCo-LDH on CFP	−10	78	118	48	2
NiFe-LDH-Pt-ht/CC	−10	101	127	9	3
	−50	205			
NiS$_2$/MoS$_2$ HNW	−10	204	65	6	4
TiO$_2$ NDs/Co NSNTs-CFs	−10	108	62	30	5
	−50	195			
	−100	235			
Pt$_3$Ni$_3$ NWs/C	−10	40	/	3	6
Ni$_3$N/Pt/Ni mesh	−10	50	/	24	7
Ni$_3$FeN/r-GO	−10	94	90	10	8
NC@CuCo$_2$Nx/CF	−10	105	76	/	9
Co-N$_x$|P-GC/FEG	−10	260	115	10	10
	−20	300			
N-Ni$_3$S$_2$/NF	−10	110	/	~3	11
o-CoSe$_2$|P	−10	104	69	20	12
MoS$_2$/Ni(OH)$_2$	−10	185	73	20	13
MoS2/FNS/FeNi	−10	122	45.1	10	14
	−20	210			
Co$_1$Mn$_1$CH	−10	180	/	10	15
	−50	281			
	−100	328			
S-NiFe$_2$O$_4$/NF	−10	138	61.3	/	16
Ni-BDT-A	−10	80	70	20	17
	−100	150			
Mo$_2$N-Mo$_2$C/HGr-3	−10	154	78	50	18
	−100	361			
W-SAC	−10	85	53	~66.6	19
Ni@NC-800	−10	205	160	10	20
FeB$_2$ NPs	−10	61	102.4	24	21
	−20	82			

	−100	172			
NFN-MOF/NF	−10	87	35.2	30	22
NiFeSP/NF	−10	94	82.6	25	23
	−50	150			
Ni(OH)$_2$@CuS	−10	150	24.2	24	24
NiO/Ru@PNS	**−10**	**39**			
	−50	**94**	**75**	**80**	**This**
	−100	**124**			**work**
	−200	**157**			

Supplemental Information Note S1: Calculation of double-layer capacitance (C$_{dl}$).

The C_{dl} was used to determine the electrochemically active surface area (ECSA) of each electrode according to the reference.[25] To measure the value of C_{dl}, the potential was swept between 0.157 and 0.257 V versus the reversible hydrogen electrode (RHE) at varied scan rates. A potential range of 0.157~0.257 V was selected for the capacitance measurements because no obvious faradaic reactions can be observed in this region. The capacitive currents of $\Delta J_{|Ja-Jc}0.207@_|$ V/2 are plotted with respect to the cyclic voltammetry (CV) scan rates. The data are fitted to a line, whose slope is the C_{dl}. The C_{dl} is proportional to the surface area of electrode.

The ECSA of a catalyst can be calculated from the C_{dl} according equation S1:[2–4]

$$\mathrm{ECSA} = \frac{C_{dl}}{C_s} \qquad (S1)$$

where C_s is the capacitance of the sample of an atomically smooth planar surface of material per unit area under identical electrolyte conditions. Here we use general specific capacitance of C_s=0.04 mF cm^{-2} in 1 M KOH based on typical reported values.[26,27]

Supplemental Information Note S2: Calculation of turn over frequency (TOF).

The TOF values can be calculated by the equation $TOF = I/2nF$, where these physical variables F, n, and I are corresponding to the Faraday constant (~96485 C/mol), the number of active sites (mol), and the current (A) during the LSV measurement in 1 M KOH, respectively. The factor 1/2 is due to fact that two electrons are required to form one hydrogen molecule from two protons.

The number of active sites was determined by an electrochemical method.[28-31] The CV curves were carried out in the potential range of -0.2–0.6 V vs RHE with a scan rate of 50 mV s^{-1} in 1M PBS electrolyte (pH = 7). Due to the difficulty in assigning the observed peaks to a given redox couple, the number of active sites is nearly proportional to the integrated voltammetric charges (cathodic and anodic) over the CV curves. Supposing a one electron process for both reduction and oxidation, we can get the upper limit of the number of active sites (n) based on the equation $n = Q/2F$, where F and Q are the Faraday constant and the whole charge of CV curve, respectively. The resulting value is the number of active sites of the catalyst.

Supplemental Information Note S3: H$_2$ quantification and Faraday efficiency.

Faraday efficiencies of the HER were calculated by the ratio of the actual amount of evolved H$_2$ to the theoretical amount of H$_2$.[32,33] H$_2$ was collected by a water drainage method and its amount (in mol) was then calculated using the ideal gas law.[34,35] The theoretical H$_2$ amount is determined by assuming that 100% electrolysis efficiency. Fig. S6 shows the experimental and theoretical amounts of H$_2$ after 90 min electrolysis.

Supplemental Information Note S4: The density functional theory (DFT) Computational details.

The DFT studies were performed by using the Vienna *Ab initio* Simulation Package (VASP)[36,37] along with the projector augmented wave (PAW)[38] method. The generalized gradient approximation (GGA)[39] functional with the Perdew-Burke-Emzerhof formulation was adopted to describe the exchange-correlation interaction among electrons, and we used an energy cutoff of 450 eV for the plane wave expansion. A semi-empirical van der waals (vdW)[40,41] correction (optB86b-vdW) for the dispersion interactions was considered. More than 10 Å thick slabs with 16 Å of vacuum along the z-direction were used to model for calculation of the surface so that these systems were large enough to avoid artificial

interaction caused by periodicity. The convergence threshold was set as 10^{-5} eV per unit cell in energy and 0.05 eV/Å per atom in force. The CI-NEB[42] is applied for computing decomposition barriers, which is an improved algorithm of the traditional NEB method.
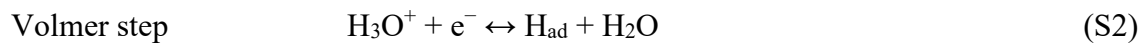
The hydrogen evolution reaction (HER) activity over a given system is correlated to the adsorption energy of a single H atom on the system. Thus, the free energy of H*, $\Delta G(H^*)$, can be considered as an effective descriptor for evaluating HER activity, which is defined as[43],
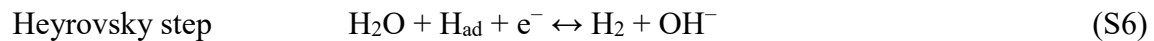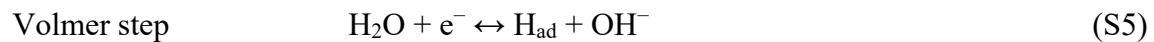
$$\Delta G(H^*) = \Delta E(H^*) + \Delta ZPE - T\Delta S$$

Where $\Delta E(H^*)$ is the binding energy of H atom and possible adsorption sites, ΔZPE is the zero point energy change of H* by using the equation of $\Delta ZPE = ZPE(H^*) - 1/2ZPE(H_2)$ with a value of $ZPE(H_2)$ = 0.230 eV. $T\Delta S$ is the entropy change of H*, which is determined to be –0.20 eV at 298 K and 1 atm.

Supplemental Information Note S5: Kinetic analysis based on the dual-pathway kinetic model.

HER kinetic analyses of Ru@PNS and NiO/Ru@PNS were performed according the procedure of Yang and Wang *et al*.[2,44-46] Based on the Volmer-Tafel-Heyrovsky mechanism, the HER/HOR on the catalysts' surfaces undergoes a multistep reaction process, which is suggested as two different mechanisms with triple possible reactions. In acidic solution, the reactions are shown as below:

Volmer step	$H_3O^+ + e^- \leftrightarrow H_{ad} + H_2O$	(S2)
Heyrovsky step	$H_3O^+ + H_{ad} + e^- \leftrightarrow H_2 + H_2O$	(S3)
Tafel step	$2H_{ad} \leftrightarrow H_2$	(S4)

In alkaline solution:

Volmer step	$H_2O + e^- \leftrightarrow H_{ad} + OH^-$	(S5)
Heyrovsky step	$H_2O + H_{ad} + e^- \leftrightarrow H_2 + OH^-$	(S6)
Tafel step	$2H_{ad} \leftrightarrow H_2$	(S7)

Because the adsorbed reaction intermediate is the same in acid and alkali, the formula of the dual-pathway model (Volmer-Heyrovsky or Volmer-Tafel) is the same for HER in both electrolytes. Based

on the two dual-pathway models, we performed kinetic analyses to evaluate the standard activation free energies for the triple elementary reaction steps of HER.

Under steady-state conditions, $d\theta/dt = 2v_T + v_H - v_V = 0$ ($2v_T + v_H = v_V$), where θ is the surface coverage of the active reaction intermediate, and v is the reaction rate. The current density is directly proportional to the sum of the reaction rates for the two single electron-transfer reactions (v_H and v_V). Thus, the total kinetic currents (j_k) can be expressed by the currents of any two elementary reactions, wherein $j_i = 2Fv_i$:

$$j_k = F(v_V + v_H) = 2F(v_T + v_H) = 2F(v_V - v_T)$$

$$= (j_V + j_H)/2 = j_T + j_H = j_V - j_T \tag{S8}$$

The kinetic currents using the activation free energies and the adsorption free energies as the adjustable parameters for each individual step are:

$$j_T = j_{+T} - j_{-T} = j^* e^{-\Delta G_{+T}^{*0}/kT}\left[(1-\theta)^2 - e^{2\Delta G_{ad}^0/kT}\theta^2\right] \tag{S9}$$

$$j_H = j_{+H} - j_{-H} = j^* e^{-\Delta G_{+H}^{*0}/kT}\left[e^{0.5\eta/kT}(1-\theta) - e^{\Delta G_{ad}^0 - 0.5\eta/kT}\theta\right] \tag{S10}$$

$$j_V = j_{+V} - j_{-V} = j^* e^{-\Delta G_{-V}^{*0}/kT}\left[e^{(\Delta G_{ad}^0 + 0.5\eta)/kT}\theta - e^{-0.5\eta/kT}(1-\theta)\right] \tag{S11}$$

where ΔG_{ad}^0 is the standard free energy of adsorption for the reaction intermediate, i.e., Had, and ΔG_i^{*0} is the standard activation free energy for the triple elementary reaction steps (ΔG_{+T}^{*0} for Tafel step, ΔG_{+H}^{*0} for Heyrovsky step, and ΔG_{-V}^{*0} for Volmer step). $kT = 25.51$ meV at 300 K.

To find the adsorption isotherm, $\theta(\eta)$, we let $g_i = e^{-\Delta G_i^{*0}/kT}$. Combing the steady-state equation, $d\theta/dt = 2v_T + v_H - v_V = 0$, with Eqs. S8-10 leads to

$$2g_{+T}(1-\theta)^2 - 2g_{-T}\theta^2 + g_{+H}(1-\theta) - g_{-H}\theta = g_{+V}\theta - g_{-V}(1-\theta) \tag{S12}$$

where

$$g_{+T} = e^{-\Delta G_{+T}^*/kT} = e^{-\Delta G_{+T}^{*0}/kT} \tag{S13}$$

$$g_{-T} = e^{-\Delta G_{-T}^*/kT} = e^{-(\Delta G_{+T}^{*0} + 2\Delta G_{ad}^0)/kT} \tag{S14}$$

$$g_{+H} = e^{-\Delta G^*_{+H}/kT} = e^{-(\Delta G^{*0}_{+H}-0.5\eta)/kT} \tag{S15}$$

$$g_{-H} = e^{-\Delta G^*_{-H}/kT} = e^{-(\Delta G^{*0}_{+H}-\Delta G^0_{ad}+0.5\eta)/kT} \tag{S16}$$

$$g_{+V} = e^{-\Delta G^*_{+V}/kT} = e^{-(\Delta G^{*0}_{-V}-\Delta G^0_{ad}-0.5\eta)/kT} \tag{S17}$$

$$g_{-V} = e^{-\Delta G^*_{-V}/kT} = e^{-(\Delta G^{*0}_{-V}+0.5\eta)/kT} \tag{S18}$$

Equation S11 can be rearranged into a quadratic equation, $A\theta^2 + B\theta + C = 0$, where

$$A = 2g_{+T} - 2g_{-T} \tag{S19}$$

$$B = -4g_{+T} - g_{+H} - g_{-H} - g_{+V} - g_{-V} \tag{S20}$$

$$C = 2g_{+T} + g_{+H} + g_{-V} \tag{S21}$$

Thus, the equations for calculating the adsorption isotherm, θ, are given below:

$$\theta = \frac{-B - \sqrt{B^2 - 4AC}}{2A} \tag{S22}$$

The kinetic current, $j_k(\eta) = f(\Delta G^{*0}_{-V}, \Delta G^{*0}_{+H}, \Delta G^{*0}_{+T}, \Delta G^0_{ad}, j^*, \theta)$, can be determined by Eqs. S8-11,

where the adsorption isotherm, $\theta(\eta) = f(\Delta G^{*0}_{-V}, \Delta G^{*0}_{+H}, \Delta G^{*0}_{+T}, \Delta G^0_{ad})$, is obtained from Eqs. S12-22.

Supplementary References:

1   J. X. Feng, J. Q. Wu, Y. Tong and G. R. Li, *J. Am. Chem. Soc.*, 2018, **140**, 610–617.
2   J. Hu, C. Zhang, L. Jiang, H. Lin, Y. An, D. Zhou, M. K. H. Leung and S. Yang, *Joule*, 2017, **1**, 383–393.
3   S. Anantharaj, K. Karthick, M. Venkatesh, T. V. S. V. Simha, A. S. Salunke, L. Ma, H. Liang and S. Kundu, *Nano Energy*, 2017, **39**, 30–43.
4   P. Kuang, T. Tong, K. Fan and J. Yu, *ACS Catal.*, 2017, **7**, 6179–6187.
5   J. X. Feng, H. Xu, Y. T. Dong, X. F. Lu, Y. X. Tong and G. R. Li, *Angew. Chem., Int. Ed.*, 2017, **56**, 2960–2964.
6   P. Wang, K. Jiang, G. Wang, J. Yao and X. Huang, *Angew. Chem., Int. Ed.*, 2016, **55**, 12859–12863.
7   Y. Wang, L. Chen, X. Yu, Y. Wang and G. Zheng, *Adv. Energy Mater.*, 2017, **7**, 1601390.
8   Y. Gu, S. Chen, J. Ren, Y. A. Jia, C. Chen, S. Komarneni, D. Yang and X. Yao, *ACS Nano*, 2018, **12**, 245–253.
9   J. Zheng, X. Chen, X. Zhong, S. Li, T. Liu, G. Zhuang, X. Li, S. Deng, D. Mei and J. G. Wang, *Adv. Funct. Mater.*, 2017, **27**, 1704169
10 Y. Hou, M. Qiu, T. Zhang, J. Ma, S. Liu, X. Zhuang, C. Yuan and X. Feng, *Adv. Mater.*, 2017, **29**, 1604480.

11   P. Chen, T. Zhou, M. Zhang, Y. Tong, C. Zhong, N. Zhang, L. Zhang, C. Wu and Y. Xie, *Adv. Mater.*, 2017, **29**, 1701584.

12   Y. R. Zheng, P. Wu, M. R. Gao, X. L. Zhang, F. Y. Gao, H. X. Ju, R. Wu, Q. Gao, R. You, W. X. Huang, S. J. Liu, S. W. Hu, J. Zhu, Z. Li and S. H. Yu, *Nat. Commun.*, 2018, **9**, 2533.

13   Z. Zhu, H. Yin, C. T. He, M. Al Mamun, P. Liu, L. Jiang, Y. Zhao, Y. Wang, H. G. Yang, Z. Tang, D. Wang, X. M. Chen and H. Zhao, *Adv. Mater.*, 2018, 1801171.

14   Y. Wu, F. Li, W. Chen, Q. Xiang, Y. Ma, H. Zhu, P. Tao, C. Song, W. Shang, T. Deng and J. Wu, *Adv. Mater.*, 2018, **30**, 1803151.

15   T. Tang, W. J. Jiang, S. Niu, N. Liu, H. Luo, Y. Y. Chen, S. F. Jin, F. Gao, L. J. Wan and J. S. Hu, *J. Am. Chem. Soc.*, 2017, **139**, 8320–8328.

16   J. Liu, D. Zhu, T. Ling, A. Vasileff and S. Z. Qiao, *Nano Energy*, 2017, **40**, 264–273.

17   C. Hu, Q. Ma, S. F. Hung, Z. N. Chen, D. Ou, B. Ren, H. M. Chen, G. Fu and N. Zheng, *Chem*, 2017, **3**, 122–133.

18   H. Yan, Y. Xie, Y. Jiao, A. Wu, C. Tian, X. Zhang, L. Wang and H. Fu, *Adv. Mater.*, 2018, **30**, 1704156.

19   W. Chen, J. Pei, C. T. He, J. Wan, H. Ren, Y. Wang, J. Dong, K. Wu, W. C. Cheong, J. Mao, X. Zheng, W. Yan, Z. Zhuang, C. Chen, Q. Peng, D. Wang and Y. Li, *Adv. Mater.*, 2018, **30**, 1800396.

20   Y. Xu, W. Tu, B. Zhang, S. Yin, Y. Huang, M. Kraft and R. Xu, *Adv. Mater.*, 2017, **29**, 1605957.

21   H. Li, P. Wen, Q. Li, C. Dun, J. Xing, C. Lu, S. Adhikari, L. Jiang, D. L. Carroll and S. M. Geyer, *Adv. Energy Mater.*, 2017, **7**, 1700513.

22   D. Senthil Raja, X. F. Chuah and S. Y. Lu, *Adv. Energy Mater.*, 2018, 1801065.

23   Y. Xin, X. Kan, L. Y. Gan and Z. Zhang, *ACS Nano*, 2017, **11**, 10303–10312.

24   S. Q. Liu, H. R. Wen, Y. Guo, Y. W. Zhu, X. Z. Fu, R. Sun and C. P. Wong, *Nano Energy*, 2018, **44**, 7–14.

25   Z. L. Wang, X. F. Hao, Z. Jiang, X. P. Sun, D. Xu, J. Wang, H. X. Zhong, F. L. Meng and X. B. Zhang, *J. Am. Chem. Soc.*, 2015, **137**, 15070–15073.

26   C. C. L. McCrory, S. Jung, J. C. Peters and T. F. Jaramillo, *J. Am. Chem. Soc.*, 2013, **135**, 16977–16987.

27   Y. Liu, X. Liang, L. Gu, Y. Zhang, G. D. Li, X. Zou and J. S. Chen, *Nat. Commun.*, 2018, **9**, 2609.

28   D. Merki, S. Fierro, H. Vrubel and X. Hu, *Chem. Sci.*, 2011, **2**, 1262-1267.

29   J. Tian, Q. Liu, A. M. Asiri and X. P. Sun, *J. Am. Chem. Soc.*, 2014, **136**, 7587-7590.

30   X. J. Liu, J. He, S. Z. Zhao, Y. P. Liu, Z. Zhao, J. Luo, G. Z. Hu, X. M. Sun and Y. Ding, *Nat. Commun.*, 2018, **9**, 4365.

31   X. J. Fan, Y. Y. Liu, S. Chen, J. J. Shi, J. J. Wang, A. Fan, W. Y. Zan, S. D. Li, W. A. Goddard and X. M. Zhang, *Nat. Commun.*, 2018, **9**, 1809.

32   Y. Sun, K. Xu, Z. Wei, H. Li, T. Zhang, X. Li, W. Cai, J. Ma, H. J. Fan and Y. Li, *Adv. Mater.*, 2018, **1802121**, 1802121.

33   L. L. Feng, G. Yu, Y. Wu, G. D. Li, H. Li, Y. Sun, T. Asefa, W. Chen and X. Zou, *J. Am. Chem. Soc.*, 2015, **137**, 14023–14026.

34   Y. Liu, Q. Li, R. Si, G. D. Li, W. Li, D. P. Liu, D. Wang, L. Sun, Y. Zhang and X. Zou, *Adv. Mater.*, 2017, **29**, 1606200.

35   H. Xu, J. Cao, C. Shan, B. Wang, P. Xi, W. Liu and Y. Tang, *Angew. Chem., Int. Ed.*, 2018, **57**, 8654–8658.

36   G. Kresse and J. Furthmüller, *Phys. Rev. B*, 1996, **54**, 11169.

37   G. Kresse and J. Furthmüller, *Comput. Mater. Sci.*, 1996, **6**, 15.

38   G. Kresse and D. Joubert, *Phys. Rev. B*, 1999, **59**, 1758.

39   J. P. Perdew, K. Burke and M. Ernzerhof, *Phys. Rev. Lett.*, 1996, **77**, 3865.

40   J. Klime, D. R. Bowler and A. Michaelides, *Phys. Rev. B Condens. Matter Mater. Phys.*, 2011, **83**, 195131.
41   J. Klimeš, D. R. Bowler and A. Michaelides, *J. Phys. Condens. Matter*, 2009, **22**, 022201.
42   G. Henkelman, B. P. Uberuaga and H. Jónsson, *J. Chem. Phys.*, 2000, **113**, 9901–9904.
43   J. K. Nørskov, T. Bligaard, A. Logadottir, J. R. Kitchin, J. G. Chen, S. Pandelov and U. Stimming, *J. Electrochem. Soc.*, 2005, **152**, J23.
44   K. Elbert, J. Hu, Z. Ma, Y. Zhang, G. Chen, W. An, P. Liu, H. S. Isaacs, R. R. Adzic and J. X. Wang, *ACS Catal.*, 2015, **5**, 6764−6772.
45   J. X. Wang, T. E. Springer and R. R. Adzic, *J. Electrochem. Soc.*, 2006, **153**, A1732–A1740.
46   J. X. Wang, T. E. Springer, P. Liu, M. Shao and R. R. Adzic, *J. Phys. Chem. C*, 2007, **111**, 12425–12433.